A FUNCTION MINIMIZATION CALCULATION OF CYCLONE 10 MAGNETIC FIELDS

S.Zaremba and Wang Liangming* (王良明)

(*Ion Beam Applications s.a., Chemin du Cyclotron 2, B-1348 Louvain-la-Neuve, Belgium*)

(Received January 1991)

ABSTRACT

By applying function minimization calculation method, two function expressions are used to simulate the magnetic field measured for cyclotron Cyclone 10 in azimuth and radius. The numerical fitting curves are consistent with magnetic field measured. In most places, the accuracies are several thousandth, except those errors to be pointed out in paper.

Keyword: Function minimization calculation MINUIT program Periodic function Seeking remainder function Fringing field Function simulation

I. INTRODUCTION

The Cyclone 10 is a compact 10 MeV proton, 5 MeV deuteron cyclotron employing negative ion technology. Its magnet consists of four symmetry sectors. The magnetic field was realized according to the proposed magnet geometry and the field calculation by the program Poisson. Fig.1 and 2 present the dimensions of magnet hill and valley respectively. The measurement of the Cyclone 10 created magnetic field map was fulfilled every 2 cm in radius and every 2° in azimuth. Table 1 presents a set of typical data of measured magnetic field in the center of a sector hill, in the center of a magnet valley and the intersection between hill and valley.

In azimuth, a function expression will be adopted to present the variation of magnetic field in order to find an equilibrium orbit for protons.

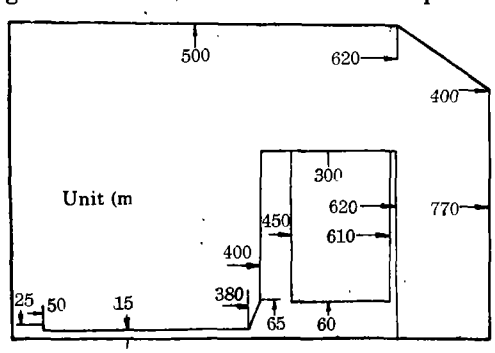

Fig.1 Poisson data, Magnetic sector

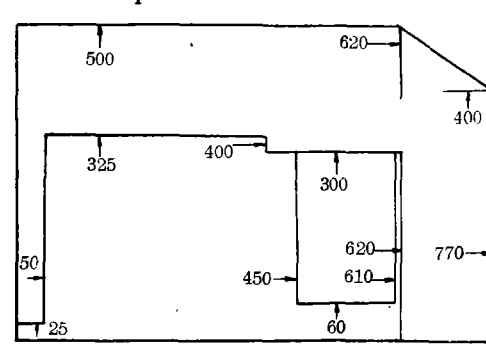

Fig.2 Poisson data, Magnetic valley

In radius, the magnetic field map has limited range, until $r=46$ cm. It is necessary to find a prolongation of the magnetic field for a greater radius r in order to calculate

* Work done at I.B.A. Wang is now at Institute of Nuclear Science and Technology of Sichuan University

the beam trajectory after stripper.

The MINUIT program was used to fit a function in with measured magnetic field.

Table 1

Typical values of magnetic field measured

Radius (cm)	B_{hill} (Gauss)	B_{valley} (Gauss)	$B_{intersection}$ (Gauss)
0	13315.7876	13314.4644	13315.5851
2	13304.8901	13265.6041	13281.7433
4	13941.7836	12755.3564	13064.4560
6	17244.1512	10502.0834	11827.1413
8	18888.9780	8283.7376	10678.9428
10	19361.6113	7039.4576	10277.0895
12	19441.8423	6231.3406	10063.3394
14	19496.5645	5631.0395	9861.6674
16	19521.2598	5159.9652	9867.3796
18	19512.1623	4773.3430	9836.9242
20	19469.2143	4450.6446	9859.7611
22	19425.9208	4173.3967	10046.7699
24	19420.6973	3942.1892	10179.9029
26	19400.1335	3741.7057	10373.5997
28	19333.9455	3561.8476	10635.1756
30	19328.7877	3407.8744	11019.1243
32	19270.9738	3262.5916	11340.4117
34	19212.1778	3120.1631	12258.2628
36	18993.9823	2963.6909	14556.6605
38	16017.3609	2786.1890	13743.4128
40	8892.6742	2582.5269	7949.0578
42	5397.3368	2360.8032	4909.1273
44	3740.5704	2129.4251	3429.4484
46	2796.5480	1886.5607	2588.4418

It offers a possibility within one program of catering to different kinds of function since it incorporates three different minimization methods. The three minimizing methods are SEEK (a Monte Carlo searching subroutine), SIMPLEX (a minimizing subroutine using a method by Nelder and Mead) and MIGRAD (a minimizing subroutine based on a variable metric method by Fletcher). The last two methods are mainly used to fit the measured magnetic field.

II. RESULTS

In azimuth, a good periodic function is used to calculate the approximate values from the formula given below: $B_z = B_0 [1 + f\cos \varphi /(1 - k^2\sin\varphi)^{1/2}]$, where $\varphi = \text{sig } n(\theta) \cdot \pi \cdot (|\theta|/\pi)^n$, $\theta \in [0,\pi]$, $\varphi \in [0,\pi]$. φ changes its linearity values from $-\pi$ to π every $\pi/4$ range when n equals 1. In subroutine FCN, a seeking remainder function was used to extend the range from $[0,\pi]$ to $[-2\pi, 2\pi]$ in a clever way.

So that the approximation of B_z will be determined by four variables B_0, f, k and n.

Table 2

Fitting values of four parameters in azimuth

Radius (cm)	B_0 (Gauss)	f	k	n
0	13318.87	− 0.00004	0.50734	0.88374
2	13284.20	− 0.00141	0.00000	1.01525
4	13353.57	− 0.04376	0.00000	1.27048
6	13939.04	− 0.23971	0.00000	1.44142
8	13701.19	− 0.38683	0.55844	1.22646
10	13364.98	− 0.46238	0.73588	1.07487
12	13039.97	− 0.50824	0.81889	0.98637
14	12804.25	− 0.54298	0.86344	0.93559
16	12606.97	− 0.57049	0.89292	0.90046
18	12425.75	− 0.59323	0.91244	0.86987
20	12249.89	− 0.61236	0.92677	0.84191
22	12096.39	− 0.62884	0.93844	0.82026
24	11984.13	− 0.64355	0.94631	0.80359
26	11871.21	− 0.65666	0.95274	0.78602
28	11741.52	− 0.66791	0.95798	0.76938
30	11660.79	− 0.67794	0.96232	0.75611
32	11557.95	− 0.68648	0.96441	0.74461
34	11439.30	− 0.69717	0.96423	0.72175
36	11177.85	− 0.71195	0.96645	0.67533
38	9508.09	− 0.68743	0.96766	0.63948
40	5775.05	− 0.54152	0.95030	0.59315
42	3888.15	− 0.39050	0.92625	0.56533
44	2934.34	− 0.27785	0.89544	0.55891
46	2337.28	− 0.20041	0.85945	0.56485
48	1034.83	− 0.38633	0.33608	0.48631
50	173.67	− 0.99619	0.00000	0.59330
52	12.88	− 0.98765	0.60946	0.94881
54	0.20	− 0.97753	0.81226	1.17642

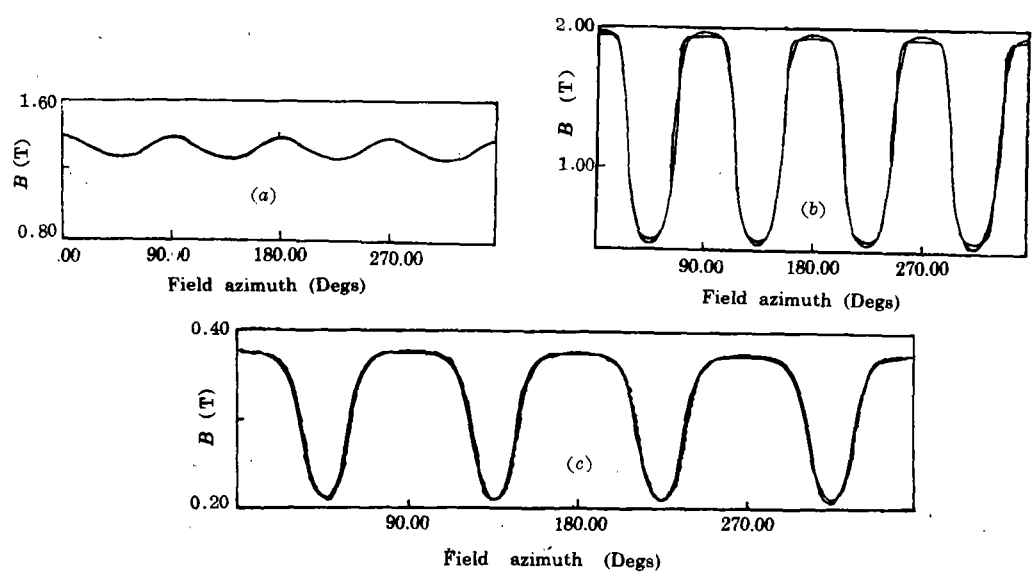

Fig.3 The azimuthal fitting curve for magnetic field at radii 4cm (*a*), 20cm (*b*) and 44cm (*c*)

The different values of four parameters will fit the azimuthal magnetic fields measured. Table 2 presents the four parameters obtained.

Table 3

Fitting values of six parameters in radius

Angle	B_0	s_0	c_0	c_1	c_2	c_3
0°	19439.42	57.47469	23.06486	13.61601	2.95428	0.22183
2°	19435.05	57.65264	23.89097	13.97272	2.99426	0.22183
4°	19427.07	57.51329	23.17616	13.64735	2.95254	0.22102
6°	19413.84	57.62843	23.88601	13.99300	3.00318	0.22282
8°	19398.00	57.67292	23.98641	14.01147	2.99780	0.22171
10°	19372.56	57.66314	24.01335	14.03670	3.00469	0.22232
12°	19327.08	57.50764	23.56740	13.89827	3.00530	0.22470
14°	19280.63	57.55123	23.88273	14.05664	3.02980	0.22572
16°	19219.78	57.33865	22.83645	13.58702	2.97234	0.22506
18°	19108.23	57.18434	21.99307	13.18198	2.91560	0.22350
20°	18897.55	56.50615	20.10451	12.52414	2.89961	0.23317
22°	18396.24	55.72636	18.87129	12.40486	3.03693	0.25816
24°	17398.92	54.18218	14.56793	10.64406	2.96277	0.28791
26°	14525.69	53.84853	10.61900	7.38983	2.04299	0.20532
28°	8834.99	52.62314	9.40222	8.56439	2.93156	0.35743
30°	7344.70	52.03515	8.05201	7.75368	2.74732	0.34788
32°	5462.94	52.03990	6.46982	6.42813	2.27240	0.29328
34°	4629.69	50.08749	3.67099	4.81336	2.08721	0.33299
36°	4087.71	48.91041	2.31485	4.04203	2.07839	0.38628
38°	3735.84	47.98553	1.28103	3.21103	1.96142	0.42663
40°	3514.90	47.73883	1.02059	3.07681	1.99714	0.45182
42°	3392.66	47.53211	0.80251	2.89141	1.97538	0.46522
44°	3351.97	47.07708	0.39868	2.34682	1.78661	0.46989
46°	3387.26	47.45612	0.73072	2.80218	1.94708	0.46645
48°	3504.06	47.67613	0.95951	3.01658	1.98385	0.45433
50°	3717.76	47.93386	1.23299	3.18274	1.96346	0.43043
52°	4059.06	48.80952	2.20947	3.97818	2.07713	0.39141
54°	4586.70	49.98905	3.58655	4.79760	2.10217	0.33824
56°	5395.93	51.92347	6.40346	6.45245	2.29691	0.29822
58°	7237,25	52.52060	8.14052	7.39770	2.48395	0.30005
60°	8677.87	52.27402	8.33703	7.80937	2.77649	0.35411
62°	14371.91	53.09655	10.93138	7.49983	2.03137	0.20000
64°	17354.45	54.36021	15.15206	10.95711	3.00286	0.28686
66°	18360.56	55.84622	19.77698	12.94400	3.13713	0.26344
68°	18904.02	56.55639	20.61257	12.90404	2.97629	0.23802
70°	19122.19	56.82720	21.08258	12.91051	2.92567	0.22988
72°	19234.40	57.49136	23.64559	13.96723	3.02294	0.22615
74°	19292.49	57.57123	23.92913	14.07477	3.03026	0.22543
76°	19333.68	57.64127	24.16086	14.15763	3.03430	0.22465
78°	19377.93	57.67416	24.02455	14.04511	3.00552	0.22224
80°	19405.04	57.71705	24.04051	14.01677	2.99174	0.22066
82°	19422.07	57.85534	24.35567	14.08350	2.97885	0.21770
84°	19433.95	58.04919	24.98732	14.27140	2.97616	0.21440
86°	19441.79	58.00092	24.98175	14.33544	3.00282	0.21719
88°	19445.91	57.90994	24.73829	14.27940	3.01056	0.21917

Fig. 3 presents the typical fitting curves of the magnetic field at three different

radii. The small wave line is the fitting curve and the smooth one is the magnetic field measured.

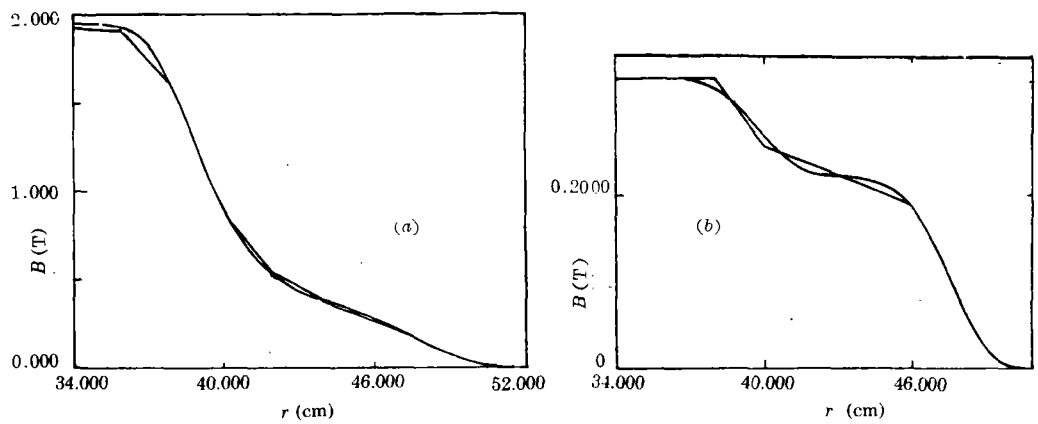

Fig.4 A prolongation curve of the fringing field for a hill (*a*) and a valley (*b*)

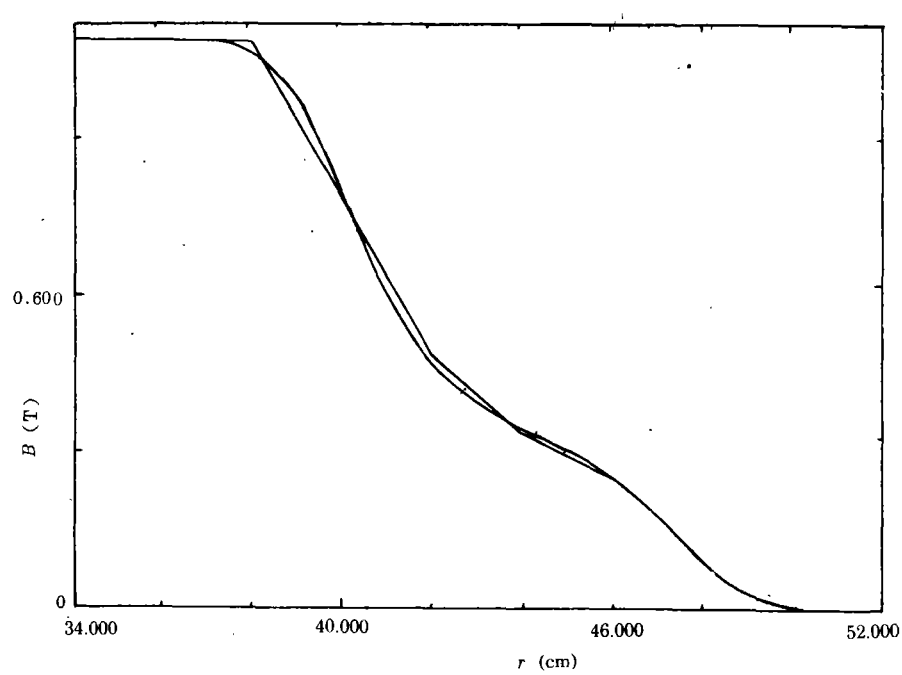

Fig.5 A curve of the fringing field between hill and valley

In radius, another function is adopted to construct the fringing field.

$$B_z = B_0/[1+\exp(s_1)]$$

$$s_1 = c_0 + c_1 s + c_2 s^2 + c_3 s^3$$

s is a function of radius r, the gap between magnet poles and a variable hard edge value s_0. So that the different values of six variables B_0, s_0, c_0, c_1, c_2 *and* c_3 will fit the

measured magnetic fields and construct the prolongations of the fringing magnetic fields in radius. Table 3 presents the six parameters obtained from the symmetry axis of a sector to another one.

Several different methods were chosen to fit the fringing fields and to find their prolongations due to the different shapes of the magnetic fields for hill, valley and their intersection.

In the magnet hill region, the biggest magnetic field in radius was assumed to be the highest point of the fitting curve. In the valley region the mean value of magnetic field from radius 24 cm to 38 cm and in the intersection region the mean value method of several terms before radius 36 cm were also assumed to be the highest points.

Fig. 4 and 5 present the typical fitting and prolongation curves of the fringing field for a hill 0°, a valley 44° and a intersection 26° between hill and valley. The broken line is the magnetic field measured and the curve is the fitting map and its prolongation.

The good quality of azimuthal fitting function was used again to consummate the fringing field curves because the variation of the prolongation in azimuth has a little oscillation.

III. CONCLUSIONS

Function simulation of magnetic field is an approximation and usually there is a certain discrepancy between measured magnetic fields and the fitting results. It is not possible to fit completely the function in with the measured magnetic fields without a difference. On the other hand, in most places of magnet the accuracies are several thousandth, except those errors to be pointed out here.

1) Results described above present that it will be possible to fit a good function in with the measured magnetic field of Cyclone 10. It would be convenient to find the equilibrium orbit for protons and to calculate the trajectory after stripper; 2) In azimuth, as you see, the fitting curve is very near the measured magnetic field. In the center region and the edge region of megnet, the accuracies are within 1 percent. But the difference between the fitting value and the measured magnetic field increases with amplitude increment of magnetic field. In the top of curve the accuracy is within 1.5 percent and 6 percent in the bottom; 3) In radius, the curve obtained is also near the measured magnetic field and with azimuthal variation. In edge region, the biggest difference between the fitting value and measured magnetic field is 2.5 percent in hill and intersection, 4 percent in valley; 4) Comparing with the data obtained by POISSON program, the prologation of the fringing field in radius drops down a little fast. The variation of the prolongation in azimuth has a little oscillation in intersection region between hill and valley.